



Termodinámica



EXERGETIC ANALYSIS OF A REFRIGERATION SYSTEM

ANÁLISIS EXERGÉTICO DE UN SISTEMA DE REFRIGERACIÓN

J. M. Belman-Flores*, A. Gallegos-Muñoz, J. M. Riesco-Ávila, A. Zaleta-Aguilar, J. M. Mendoza-Miranda
Department of Mechanical Engineering, Engineering Division, Campus Irapuato-Salamanca, University of Guanajuato, Salamanca, Gto., Mexico.

Received March 4, 2014; Accepted October 4, 2014

Abstract

This paper presents the exergy analysis of an experimental refrigeration system that operates with the refrigerant R134a. The research is based on analyzing the influence of six operational and controllable parameters of the experimental setup such as the compressor frequency of operation, the degree of static superheat, and the temperature of the secondary fluids (at the inlet of the evaporator and the condenser) on the exergy destruction. Thus, the results show that most exergy destruction is located in the condenser, followed by the compressor, the expansion valve and the evaporator. Furthermore, the highest exergetic efficiency is obtained by a decrease in the temperature of the secondary fluid inside the evaporator, and by an operation of the compressor at low speed. The efficiency of the compressor is also included in the analysis, which is a parameter that determines the exergy destruction of the largest component. Finally, a function of the exergetic efficiency is established in order to find those magnitudes of operational parameters that contribute to improving this efficiency.

Keywords: irreversibilities, vapor compression, exergy, R134a, controllable parameters, combined efficiency.

Resumen

En este trabajo se presenta el análisis exergético de un sistema experimental de refrigeración que trabaja con el refrigerante R134a. El trabajo desarrollado analiza la influencia de seis parámetros operacionales y controlables de la instalación experimental como: la frecuencia de operación del compresor, el grado de sobrecalentamiento estático y la temperatura de los fluidos secundarios (a la entrada del evaporador y condensador), sobre la destrucción de exergía. Así pues, los resultados muestran que la mayor destrucción de exergía es localizada en el condensador seguida por el compresor, la válvula de expansión y el evaporador. Por otro lado, la eficiencia exergética más alta es obtenida mediante un decremento de la temperatura del fluido secundario en el evaporador, además de un manejo bajo de la velocidad del compresor. También en el análisis se involucra la eficiencia combinada del compresor, la cual resulta en un parámetro que determina el componente con mayor destrucción de exergía. Asimismo, se establece una función de la eficiencia exergética para la búsqueda de aquellas magnitudes de los parámetros operacionales que contribuyan a mejorar dicha eficiencia.

Palabras clave: irreversibilidades, compresión de vapor, exergía, R134a, parámetros controlables, eficiencia combinada.

*Autor para la correspondencia. E-mail: jfbelman@ugto.mx

1 Introduction

Refrigeration systems are extremely important in daily life, especially in terms of preserving food, health, and comfort. Nowadays, a large number of refrigeration systems are based on vapor compression systems, which currently represent 10% of the total energy demand (Dubey *et al.*, 2010). The escalating cost in energy and its inefficient use, the indirect contribution in greenhouse gases emitted in the atmosphere, among other parameters, were the issues that trigger the improvement of the performance of vapor compression systems. Performance and optimization of such systems can be carried out using either energy or exergy analyses. Due to the fact that exergy analysis is a thermodynamic technique based on the second law of thermodynamics, it provides an alternative when comparing processes and systems rationally and meaningfully (Dinçer and Kanoğlu, 2010). An exergy analysis is usually aimed to determine the maximum performance of the system and to identify sites of exergy destruction. In the literature review of this area, there are numerous works dealing with exergy analysis of compression refrigeration and air conditioning systems. Yumrutaş *et al.*, (2002) developed a computational model based on exergy analysis for studying the effects of evaporating and condensing temperatures on pressure losses, exergy losses, second law efficiency, and the coefficient of performance, *COP*, of a vapor compression system that works with ammonia. Their results showed that the second law efficiency and *COP* increase, and exergy losses decreased when the temperature difference between the evaporator and refrigerated space was decreased. Su and Chen (2006) presented a theoretical study of exergetic efficiency optimization of a Carnot refrigeration system with multiple irreversibilities, namely finite-rate heat transfer, the internal dissipation of the working fluid, and the heat leak between the heat reservoirs. As a result of this research, they derived the maximum exergetic efficiency, and observed that it occurs when the temperature ratio between cold side and hot side processes is slightly lower than that of the temperature ratio of the two reservoirs. Chen and Su (2005) reported an optimization of the exergetic efficiency for a theoretical irreversible Brayton refrigeration cycle. The efficiency optimization was implemented by considering the isentropic temperature ratio, and the allocation factor of the thermal conductance as parameters. The maximum exergetic efficiency occurs when the isentropic temperature ratio is slightly

greater than the temperature of the two reservoirs. They concluded that the method of exergetic efficiency optimization is an important and effective criterion for the evaluation of a refrigeration cycle. Arora and Kaushik (2008) presented a theoretical performance analysis of the R502 and its substitutes (R404A and R507) based on energy and exergy concepts. The parameters computed were *COP*, exergy destruction, exergetic efficiency, and efficiency defects in the system. Ahamed *et al.*, (2011) reviewed the exergy analysis of a vapor compression system and summarized the main parameters that affect exergy, namely evaporating temperature, condensing temperature, sub-cooling, and compressor pressure. Kizilkan *et al.*, (2010) presented an exergy analysis for an experimental variable-speed system working with R404A in order to determine irreversibility rates and exergy efficiencies of each system component as well as the overall system. Their results showed that the major irreversibility occurred in the compressor followed by the condenser, the evaporator, and the expansion valve for different compressor frequencies. However, they do not explore any other parameter besides the drive frequency, such as volumetric flow and inlet temperatures for secondary fluids in both, the evaporator and the condenser. Aprea *et al.*, (2003) performed an exergy analysis of a vapor compression refrigeration plant while the refrigeration capacity was controlled by varying the compressor speed. They evaluated the complete plant and its individual components to pinpoint the greatest contribution to the decrease of the exergy performance. They proposed and tested three working fluids R407C, R507, and R417A. The authors concluded that the best performance was related to R407C, and the contribution of the compressor to the overall irreversibility was the most relevant. In this context, Kalaiselvam and Saravan (2009) applied exergy analyses to different scroll compressors using R22, R417A, and R407C to determinate the total exergy losses. The eco-friendly refrigerant R417A can be used as an alternative rather than R407C in order to preserve the exergy loss. Padilla *et al.*, (2010) followed an exergy approach in order to evaluate the thermodynamic performance of R413A in an unmodified R12 domestic refrigerating system. They carried out twelve experimental tests in a controlled environment during the selected cooling process from evaporator outlet temperature, ranging between 288[K] to 263[K] by varying the evaporator and condenser air-flows to simulate different working conditions. Their results showed that the overall

energy and exergy performance of the system working with R413A is consistently better than that of R12. Lugo-Leyte *et al.*, (2013) developed a thermodynamic and exergetic analysis applied to vapor compression refrigeration cycle with refrigerant R134a. They obtained the irreversibilities of each equipment, the exergetic operation cost in function of the environmental temperature and the temperature of the refrigerated spaced.

The main purpose of this paper is to evaluate the exergy destruction and exergetic efficiency of the complete refrigeration plant using an experimentally validated coupled model. The analysis takes into account the variation of key parameters easily obtained and controlled, such as the compressor drive frequency, superheating degree, secondary volumetric flow rates, and secondary fluid inlet temperatures. All of those variables enable a better understanding of the influence from the parameters present in a refrigeration system as opposed to analyzing only the effect of compressor drive frequency as in the literature. Finally, a maximization of exergetic efficiency is implemented to determine the best combination of controllable parameters, which improves the exergy performance of the refrigeration plant.

2 Description of the experimental plant

The vapor compression refrigerator used for developing the exergy analysis is shown in Fig. 1. The experimental plant basically consists of a vapor compression circuit and two secondary fluid circuits: the condensing water loop and a heat load simulation system. This experimental plant can work with the refrigerant R134a. The main components of the vapor compression refrigerator are: an open type reciprocating compressor, a shell and tube condenser, an expansion valve, and a shell and tube evaporator. In the shell and tube condenser, there is refrigerant flowing along the shell and water flowing inside the tubes (as secondary fluid). In contrast, in the shell and tube evaporator the refrigerant flows inside the tubes, and brine water-propilenglycol (50/50% by volume) flows in the shell. The load simulation system consists of a tank with an electrical resistance and a variable speed pump to control the thermal load of the evaporator. The condensing system is used to set the water conditions at the condenser using a commercial chiller that has a variable speed

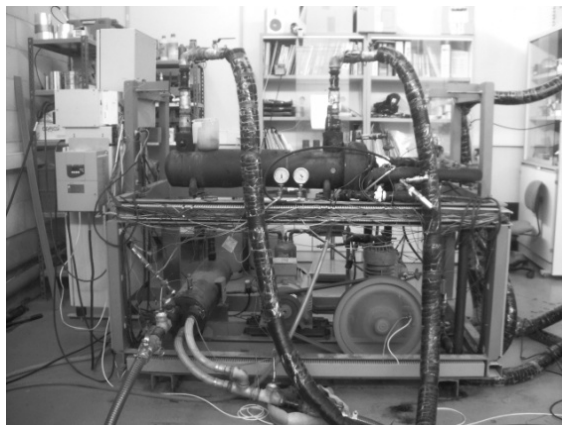


Fig. 1. Vapor compression plant.

pump. With these two systems it is possible to control the secondary fluid conditions at the evaporator and condenser. The experimental setup is fully instrumented with sensors to measure key variables such as: pressure, temperature, volumetric and mass flow rate, compressor drive frequency and energy consumption. The signals generated by all sensors, as well as those provided by the measuring devices, are gathered by a National Instruments data acquisition system.

Fig. 2 shows both the schematic and the P-h diagram of the refrigeration system. The vapor compression process begins when the refrigerant is compressed until it reaches the condensing pressure (process 7-1). Before the compressed refrigerant enters the condenser inlet, heat transfer to the environment is carried out through the discharge line and the oil separator areas causing a desuperheating of refrigerant vapor (process 1-2). The refrigerant vapor is then condensed by removing the heat through the secondary fluid into the condenser until the refrigerant reaches a subcooled condition. After the condenser, the liquid refrigerant has an extra subcooling, SC , measured in states 3 and 4. The liquid refrigerant enters the expansion valve where it expands to the evaporating pressure (process 4-5). At the evaporator, refrigerant cools the brine water-propilenglycol (process 5-6). Finally, after the evaporator, the refrigerant is superheated, SS , measured in states 6 and 7.

3 Exergy analysis

In thermodynamics, the exergy of a system is defined as the maximum work possible during a process that

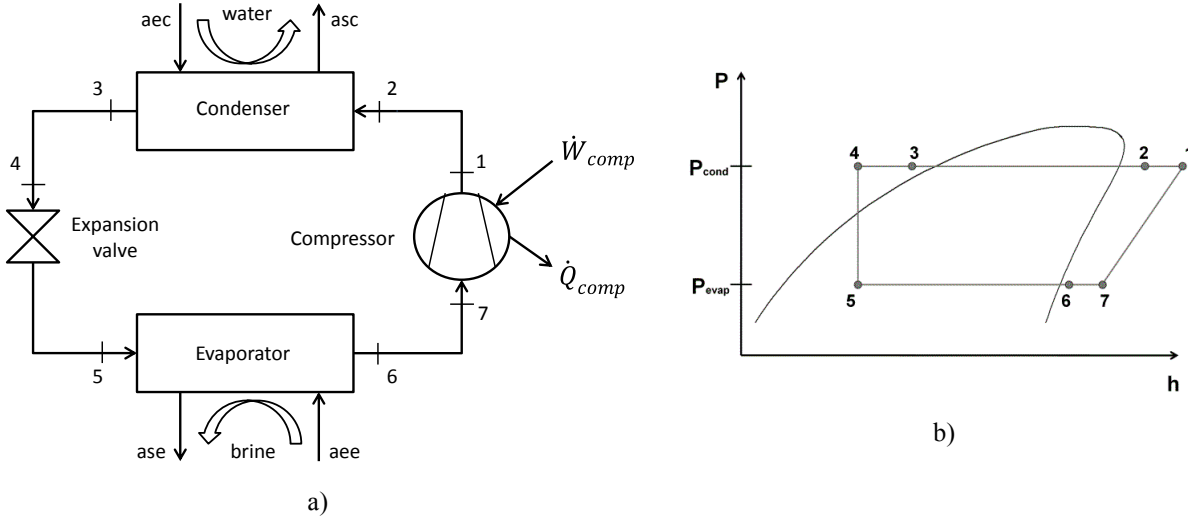


Fig. 2. a) Schematic diagram of a single-stage refrigeration system and b) P-h diagram of the single-stage refrigeration system.

brings this system into equilibrium with the environment conditions (Kotas, 1995). When the system and its environment reach equilibrium, the exergy of the system will be zero. The method of the exergetic analysis is based on the second law of thermodynamics and enables the designers to identify location, the cause and the magnitude of losses in the thermal systems. In the exergy balance, the destroyed exergy represents the real loss in the quality of energy that cannot be identified by means of the energy balance, since a conservation of energy is always considered (Tsatsaronis, 1993). The exergy analysis has been used by many authors to perform the evaluation of the efficiency of refrigeration systems (Srinivasan et al., 2003; Tao et al., 2010; Fábrega et al., 2010). Thus, the exergy analysis is a thermodynamic tool that can be used to evaluate the performance of refrigeration system by determining the magnitude and location of the process irreversibility (losses of energy quality), making it possible to study the changes of operational parameters of the process.

By applying the first and second laws of thermodynamics, the general expression of exergy balance in any system is (Moran and Shapiro, 2007):

$$\sum \left(1 - \frac{T_0}{T}\right) \dot{Q} - \dot{W} + \sum_{in} \dot{m}\psi - \sum_{out} \dot{m}\psi - \dot{E}_d = 0 \quad (1)$$

The first term of Eq. (1) takes into account all heat transfer interactions of the system with its surroundings through the boundary at temperature T . The second term is the exergy interaction by work.

The third and fourth terms are the exergy due to the fluid flow crossing the system boundaries. Finally, the fifth term measures the irreversibilities in the system analyzed.

The potential work or exergy of a fluid flow neglected the change in kinetic and potential energy is expressed as:

$$\psi = h - h_0 - (T_0)(s - s_0) \quad (2)$$

In Eq. (2) enthalpy and entropy are measured with respect to a dead state at 101.3[kPa] and 298.15[K]. The general exergetic efficiency is defined as:

$$\eta_{II} = 1 - \frac{\text{Exergy Destroyed}}{\text{Exergy Supplied}} \quad (3)$$

The exergy destruction rate in each system component is calculated using eqs. (4-8).

Compressor. The exergy balance applied to the compressor, taking into account the exergy transferred to the surroundings by heat transfer, and according to Fig. 2 is:

$$\dot{E}_{d,comp} = \dot{W}_{comp} - \left(1 - \frac{T_0}{T_{w,comp}}\right) \dot{Q}_{comp} + \dot{m}_{ref}(\psi_7 - \psi_1) \quad (4)$$

where temperature $T_{w,comp}$ is the boundary temperature located at the wall of the compression chamber of the compressor, which is defined as an average obtained through thermal images of the compressor (see Fig. 3). The value is 350.65 [K] (77.5 [°C]).

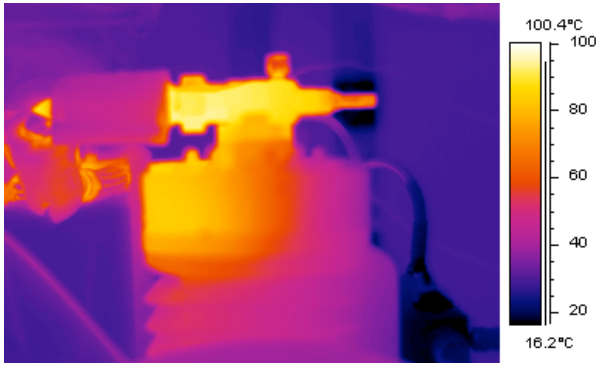


Fig. 3. Infrared thermal image of the test facility compressor.

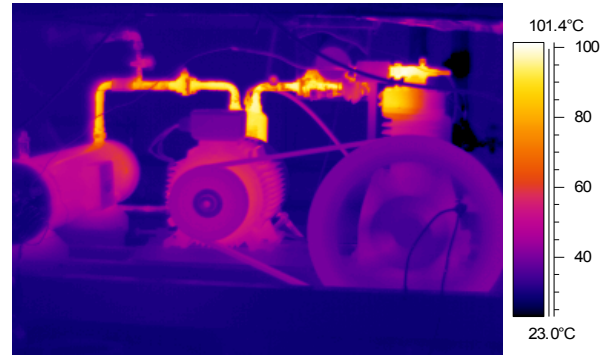


Fig. 4. Infrared thermal image of the discharge line.

Discharge line. Considering that the boundaries of the discharge line are the walls of the pipe, and therefore its temperature is the wall temperature, $T_{w,dl}$, the exergy balance for this component is defined as:

$$\dot{E}_{d,dl} = \dot{m}_{ref}(\psi_1 - \psi_2) - \left(1 - \frac{T_0}{T_{w,dl}}\right) \dot{Q}_{dl} \quad (5)$$

The discharge line is added into the exergy analysis in order to predict more accurately the total exergy destruction of the experimental test facility, taking into account the heat loss by the discharge line and the oil separator. Fig. 4 presents a thermal image of the discharge line and oil separator of the experimental vapor compression; the wall temperature is obtained from the discharge line model shown in Fig. 4, which only illustrates the average of wall temperature.

Condenser. Assuming negligible heat transfer to the surroundings, the exergy destruction rate at condenser is defined as:

$$\dot{E}_{d,cond} = \dot{m}_{ref}(\psi_2 - \psi_3) + \dot{m}_{aec}(\psi_{aec} - \psi_{asc}) \quad (6)$$

Expansion valve. In this device, the heat transfer to the surroundings was neglected because the dimensions of this component are relatively small.

$$\dot{E}_{d,ev} = \dot{m}_{ref}(\psi_4 - \psi_5) \quad (7)$$

Evaporator. Heat transfer is between the refrigerant and the water-propilenglycol brine stream since the evaporator is isolated from its surroundings. The exergy destruction is expressed as:

$$\dot{E}_{d,evap} = \dot{m}_{ref}(\psi_5 - \psi_6) - \dot{m}_{aee}(\psi_{b,in} - \psi_{b,out}) \quad (8)$$

The exergy change for brine water-propilenglycol

(assuming no pressure drop) is:

$$\psi_{b,in} - \psi_{b,out} = C_{p,b} \left[(T_{aee} - T_{ase}) - (T_0) \ln \left(\frac{T_{ase}}{T_{aee}} \right) \right] \quad (9)$$

The overall exergy destruction for the vapor compression system is defined as the individual contribution of each system component:

$$\dot{E}_{d,total} = \dot{E}_{d,comp} + \dot{E}_{d,dl} + \dot{E}_{d,cond} + \dot{E}_{d,ev} + \dot{E}_{d,evap} \quad (10)$$

Therefore, the second law efficiency for the refrigeration system is:

$$\eta_{II,cycle} = 1 - \frac{\dot{E}_{d,total}}{\dot{W}_{comp} + \dot{m}_{aec}\psi_{aec} + \dot{m}_{aee}\psi_{aee}} \quad (11)$$

Eqs. (1-11), for the exergetic analysis of the refrigeration system are incorporated to the experimental validated model by using the software EES®. This model is based on mathematical expressions which come from fundamental physics and empirical correlations established on the basis of an experimental test. The validation of the model was performed using R134a for a wide range of operating conditions of the test bench. For more details and information on this model (Belman *et al.*, 2010). Table 1 presents the range for each controllable parameter in the experimental plant. Also, the table shows information about operating parameters: the evaporating and condensing temperatures, the refrigerant temperature at the compressor outlet, the compressor power and cooling capacity. The operational parameters depend on the controllable parameters.

In order to find controllable parameters that achieve a maximum exergetic efficiency of the cycle,

and according to the topological structure proposed in the physical model by Belman *et al.*, (2010), it is possible to include an expression involving the exergetic efficiency of the cycle in correlation to the controllable parameters. Thus Eq. [12] represents the variable which is going to be maximized, and it is also programmed in the EES. The method used to solve the optimization is the Conjugate Directions method, in which the maximum number of times in equations are solved, which may be specified, along with the relative tolerance. The basic notion behind this method is to use a one-dimensional series of searches to locate the optimum which is a function, in this case, of the parameters: $f, C_{aec}, C_{aee}, T_{aec}, T_{aee}, SS$, (Belegundu and Chandrupatla, 2011).

$$\max(\eta_{II,cycle}) = g(f, C_{aec}, C_{aee}, T_{aec}, T_{aee}, SS) \quad (12)$$

Eq. (12) assumes that the exergetic efficiency can be evaluated as a function of the controllable parameters presented in table 1.

4 Results and discussion

In order to analyze the effect of controllable parameters on the exergy destruction in different component, five parameters are kept constant and one is varying within its operational range. Thermodynamics properties of all the streams of the process necessary for the calculation of the destroyed

exergy in the cycle, were obtained using the software EES. Fig. 5 shows the behavior of the exergy destruction rate when varying the compressor drive frequency between 35 to 50 [Hz], this behavior is based on fixed controllable parameters. The compressor and the condenser are the two components with major exergy destruction rate followed by the expansion valve and evaporator, respectively. When examining in detail Fig. 5, the rate of exergy destruction at the compressor is 0-12% higher than obtained at the condenser when varying the drive frequency from 35 to 41 [Hz]. However, when the compressor drive frequency is greater than 41 [Hz] the condenser exergy destruction rate becomes greater than the compressor by 0-13%. The decrease of exergy destruction after 41 [Hz] is due to a smaller entropy change in the compressor process. The exergy destruction at the expansion valve is about 0-8% higher than the evaporator. Similar tendencies to those are reported by Aprea *et al.*, (2003). The compressor exergy destruction rate has this behavior due to mechanical and electrical losses because the motor and the transmission are connected to the compressor, which defines the combined efficiency. Therefore, the exergy destruction in the compressor is caused by the refrigerant vapor that is warm at the inlet of the cylinder, the imperfection of the padding between the piston and the cylinder, and the losses in the suction and discharge valves.

Table 1. Practical parameter ranges in refrigeration plant.

Controllable parameters	
Volumetric flow of water (condenser) [m ³ h ⁻¹]	0.6-1.2
Volumetric flow of water-propylene glycol (evaporator) [m ³ h ⁻¹]	1.5-3.0
Static super heating degree [K]	5-9
Evaporator input temperature (brine) [K]	280.15-290.15
Condenser input temperature (water) [K]	288.15-303.15
Frequency [Hz]	35-50
Operating parameters	
Evaporating temperature [K]	265-282
Condensing temperature [K]	313-333
Outlet compressor temperature [K]	330-370
Compressor power [kW]	1.4-3
Cooling capacity [kW]	5-9

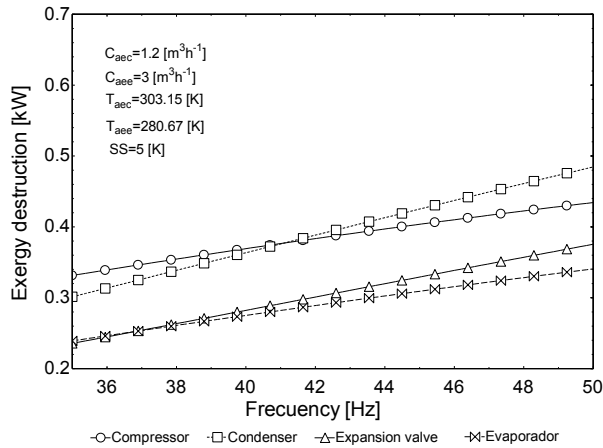


Fig. 5. Exergy destruction rate vs. compressor drive frequency.

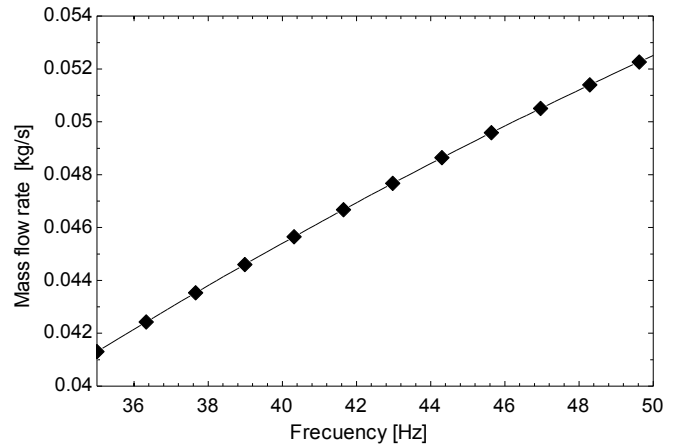


Fig. 6. Mass flow rate varying the compressor drive frequency.

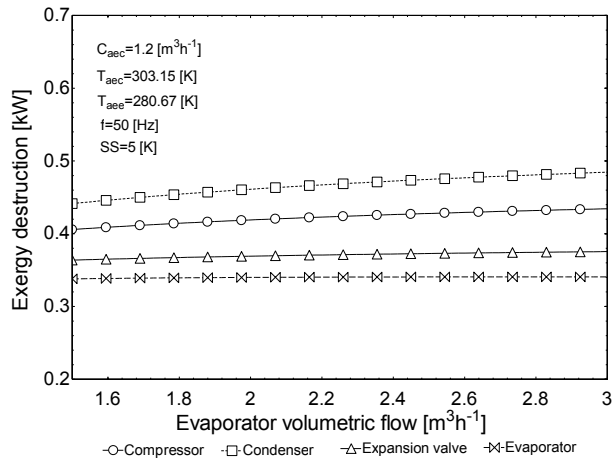


Fig. 7. Exergy destruction rate vs. volumetric flow rate at the evaporator.

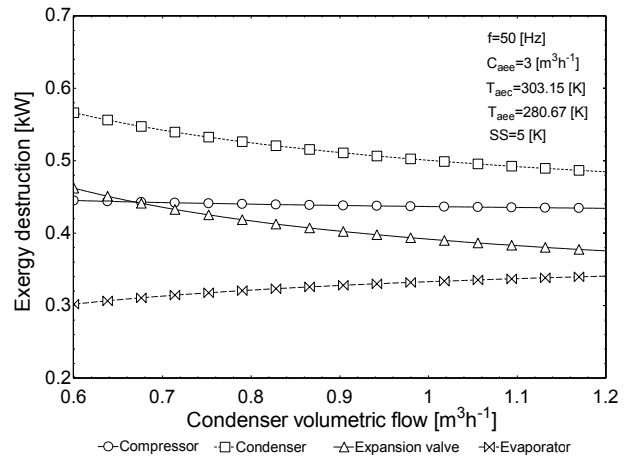


Fig. 8. Exergy destruction rate vs. volumetric flow rate at the condenser.

Thus, the real power input to the compressor depends on the state of the transmission and electrical motor driven by the compressor. So, a change in frequency, compression ratio and superheating degree, increase the exergy destruction rate. Fig. 6 shows the effect of frequency on the refrigerant mass flow rate, obviously the refrigerant mass flow rate increases with a higher frequency. Note that the frequency is within operational limits of the compressor.

The exergy destruction rate is showed in Fig. 7 when the brine volumetric flow varies between 1.5-3.0 [m³h⁻¹]. It can be observed that the condenser

presents the highest exergy destruction rate followed by the compressor, the expansion valve, and the evaporator. At the condenser, the exergy destruction rate is 0.043 [kW] while the exergy destruction rate at the compressor, the expansion valve, and the evaporator are 0.029 [kW], 0.012 [kW] and 0.003 [kW] respectively. This caused by the brine flow rate at evaporator. Increasing volumetric flow rate at the evaporator mainly increase parameters such as the refrigerant mass flow rate as well as evaporating and condensing pressures/temperatures. In this case, the lower increase observed at the evaporator (see Fig.

7) occur because the streams are close to a minimal relation of a temperature difference between the refrigerant and the brine streams, so, the volumetric flow rate has a limiting effect on exergy destruction rate.

Within the parameters that influence the refrigeration system, one of the most important is the condensing agent. Depending on the volumetric flow rate and water temperature (secondary fluid), the global system results can have a better or worse performance. Fig. 8 depicts the influence of volumetric flow of water on the exergy destruction rate in the system components. The increase in condensing agent (water) is reflected in a significant variation in both condensing and evaporating conditions, as well as a decrease in vapor quality at the evaporator inlet. This variation does not affect significantly the refrigerant mass flow rate. In the condenser, the exergy destruction rate diminishes about 0.082 [kW] due to the decrease in the condensing conditions, which are close to the reference state conditions. Furthermore, the condenser has a larger temperature difference between its streams that comes to contribute to diminish exergy destruction rate. In the compressor, the exergy destroyed practically remains constant, diminishes about 0.010 [kW] because the exergy difference between inlet and outlet is approximately the same for all range of conditions. The change in exergy destruction rate at the expansion valve decreases about 0.087 [kW]. At the evaporator, the exergy destruction rate increases because a decrease in evaporating conditions occurs, which causes that the temperature difference between refrigerant side and brine side moves away from the minimal temperature difference, this variation is about 0.038 [kW]. So, the highest exergy destruction is at the condenser, and similar result is demonstrated by Aminyavari *et al.*, (2014). With the performance shown in the above figures, it can be concluded that the volumetric flow of the secondary fluids affect slightly the exergy destruction of the components except the condenser.

Fig. 9 presents exergy destruction rate when the static superheating degree, SS, controlled by expansion valve varies between 5-9 [K]. This range was selected because superheating degree above 9 [K] diminishes the volumetric efficiency and below 5 [K] potentially affects the compressor by introducing liquid refrigerant. The variation of this parameter triggers the decrease in both the refrigerant mass flow rate and evaporating conditions at the evaporator, which implies an increase in exergy destruction rate at the evaporator. A maximum change of exergy destruction rate at evaporator is about 0.049 [kW]. At

the rest of system components the exergy destruction rate diminishes due to the decrease in the refrigerant mass flow rate. The maximum exergy destruction rate is 0.054 [kW] at the condenser, 0.071 [kW] at the compressor, and 0.023 [kW] at the expansion valve. It is observed in the figure that the exergy variations are minimal with a higher superheating degree operationally. A greater magnitude of this parameter can be achieved by adjusting the valve spindle. However in this particular installation, a greater fluctuation in the mass flow measurement of the refrigerant is perceived, therefore an appropriate value for this is 9 [K].

Fig. 10 shows the trend of the exergy destruction rate as a function of propylene glycol brine temperature at inlet of evaporator. This variation mainly increases the refrigerant mass flow rate, evaporating and condensing conditions due to its dependency on the temperature of secondary inlet fluid at evaporator which affects both evaporator and condenser. Therefore, by increasing the secondary inlet fluid temperature at the evaporator the exergy destruction rate at the condenser is of 0.242 [kW], 0.146 [kW] at the compressor, 0.057 [kW] at the expansion valve, and 0.158 [kW] at evaporator. Contrasting with the results obtained with the variation of volumetric flow rate, the variation of inlet temperature at evaporator increases drastically the temperature difference between refrigerant and secondary fluid, not only at evaporator but also in the condenser. In general, the temperature difference between the brine and refrigerant in the evaporator increases. The larger heat transfer temperature difference will lead to a larger exergy loss in the evaporator. Fig. 11 shows exergy destruction rate as a function of secondary fluid temperature condenser inlet. The increase of inlet temperature of the secondary fluid impacts the condensing and evaporating pressures/temperatures. A decrease in exergy destruction rate for both condenser and evaporator is observed due to the narrow temperature difference between the refrigerant and secondary fluid. The decrease in exergy destruction rate at the evaporator and the condenser are 0.075 [kW] and 0.127 [kW], respectively. For compressor and expansion valve the exergy destruction rate increases due to the increase in compression ratio. The increase in exergy destruction rate is 0.032 [kW] for the compressor and 0.134 [kW] for the expansion valve. From the parameter variation, it can be seen that the condenser has the greatest exergy destruction rate followed by the compressor, the expansion valve and the evaporator.

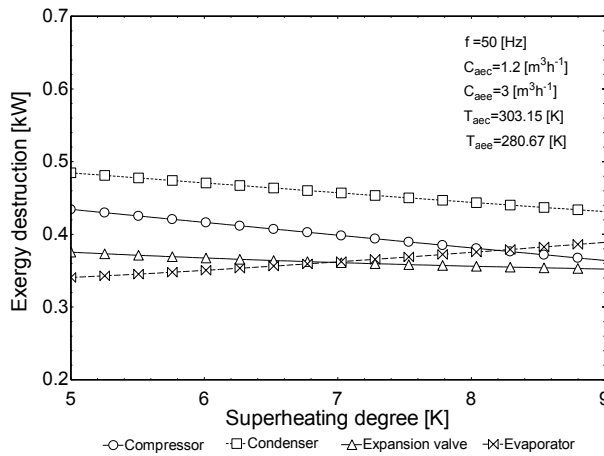


Fig. 9. Effect of superheating degree in the exergy destruction rate of refrigeration system components.

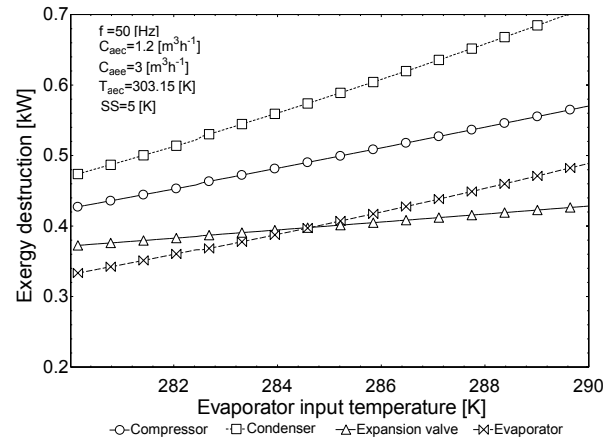


Fig. 10. Exergy destruction rate vs propylene glycol brine inlet temperature at evaporator.

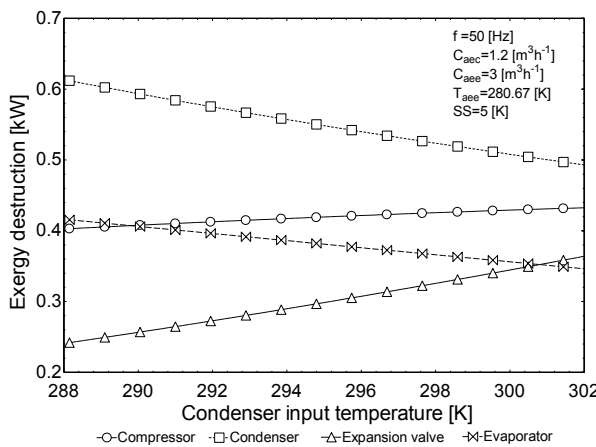


Fig. 11. Exergy destruction rate vs secondary fluid inlet temperature at condenser.

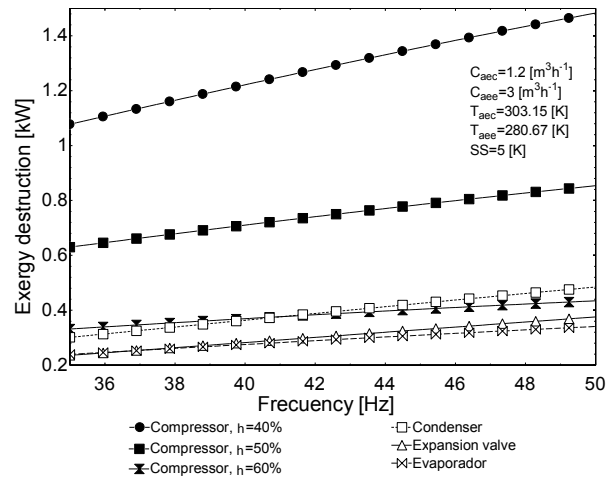


Fig. 12. Comparison of the exergy destruction rate at the system when the combined efficiency varies.

Based on the last performance (figs. 10 and 11), we conclude that the temperatures of the secondary fluids have a higher impact on the exergy destruction of the various components, and thus, this represents control parameters of great importance in the search for better exergetic performance.

To go further about the effect of the compressor on the exergy destruction in the system, it is necessary to involve its combined efficiency. The combined efficiency includes the electromechanical and transmission inefficiencies as well as the inefficiencies that occur inside the compressor as a

result of friction. So, when the combined efficiency decreases, the irreversibility at compressor increases as it is shown in Fig. 12. So, the highest exergy destruction rate is located at the compressor when combined efficiency decreases from 60% to 40%. Therefore, the exergy destruction rate at the compressor depends on other parameters such as the transmission system and the heating in the compressor. For instance, the increase in exergy destruction rate at the evaporator increases more than 90% when the combined efficiency decreases to 40%.

Finally, Fig. 13 shows the exergetic efficiency

versus the compressor drive frequency in order to determine the influence of varying controllable parameters. The changes in secondary volumetric flow rates do not have a significant influence in exergetic efficiency of the cycle. When the static superheating degree increases, the exergetic efficiency decreases about 10% with high compressor drive frequency. When increasing the inlet temperature at evaporator to 290.15 [K], the exergetic efficiency decreases about 40% compared with the minimum evaporator input temperature 280.15 [K]. The change in evaporator input temperature is the most represented variation in the exergetic efficiency of vapor compression system. The increase in inlet temperature of condensing agent proved a slight rise in exergetic efficiency, because at a high inlet temperature of secondary flow rate the

exergy difference at the condenser diminishes, and the exergetic efficiency increases.

When intending to propose new controllable parameters the major objective is the reduction of the exergy destruction. Table 2 shows the controllable parameters which an achieved higher efficiency. The optimum values shown in the table were obtained using the Eq. [12]. These parameters are only indicative of operating conditions in which the refrigeration system runs with the best exergetic efficiency, but as it is known, it is always necessary to satisfy a certain thermal load (cooling capacity), also the condenser inlet temperature depends largely on prevailing environmental conditions. Therefore these values represent only a reference state.

Table 2. Optimum controllable parameters for the experimental refrigeration plant.

Volumetric flow of water (condenser) [m ³ h ⁻¹]	0.9071
Volumetric flow of water-propylene glycol (evaporator) [m ³ h ⁻¹]	1.5
Static superheating degree [K]	9
Evaporator input temperature (brine) [K]	280.15
Condenser input temperature (water) [K]	303.15
Frequency [Hz]	35

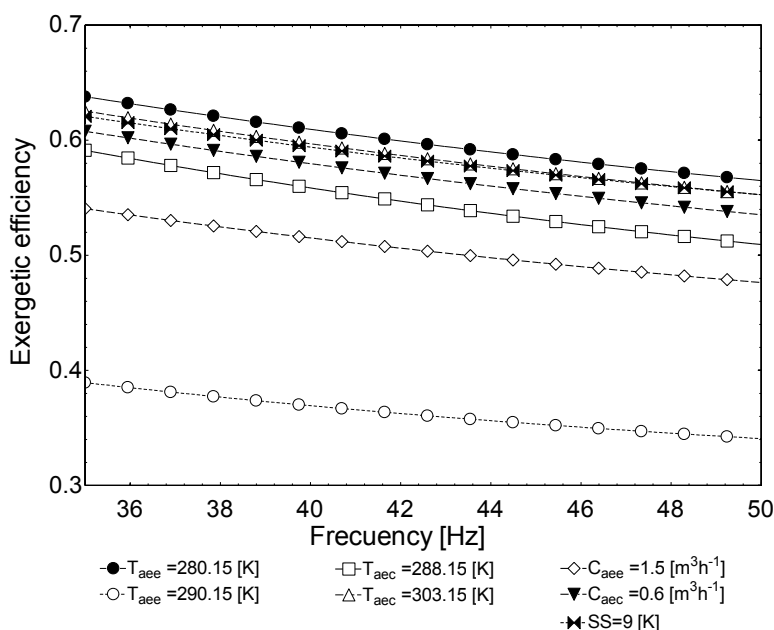


Fig. 13. Exergetic efficiency of refrigeration system varying the controllable parameters.

Conclusions

In this paper an exergetic analysis of an experimental refrigeration system using the refrigerant R134a was performed to identify and quantify the exergetic losses. This analysis shows the behavior of exergy destruction rate under the influence of controllable parameters that are easily accessible in such facilities: compressor drive frequency, volumetric flow rate and the temperature of the secondary fluids (water and brine), and the static superheating degree. Also, the analysis includes the influence of the combined efficiency of the compressor on the global system.

Through the exergetic analysis it was observed that the major exergy destruction rate is located at condenser followed by the compressor, the expansion valve, and the evaporator. The temperature of the secondary fluids, and to a lesser extent, the volumetric flow rate are the parameters which most significantly influence the exergy destruction. The contribution of the compressor to the overall irreversibility is the most relevant, its frequency driven and combined efficiency were the parameters considered in this analysis. The variation in combined efficiency depends on conditions of the transmission system, the heat transfer rate in the compressor, among others. By applying the simple Conjugate Directions method, the optimum controllable parameters that represent the maximum exergetic efficiency of the cycle were found. It is relevant to say that changes of controllable parameters require also a specific study such as the use of an optimization method (for instance, thermoeconomic methodology). Finally, it is concluded that the exergy analysis is essential for the refrigeration system.

Nomenclature

C	volumetric flow rate [m^3h^{-1}]
C_p	specific heat [$\text{kJkg}^{-1}\text{K}^{-1}$]
f	frequency [Hz]
h	specific enthalpy [kJkg^{-1}]
\dot{m}	mass flow rate [kg s^{-1}]
\dot{Q}	heat transfer rate [kW]
s	specific entropy [$\text{kJkg}^{-1}\text{K}^{-1}$]
SS	superheating degree [K]
T	temperature [K]
T_0	dead state temperature [K]
\dot{W}	power [kW]
η_{II}	exergetic efficiency
\dot{E}_d	exergy destruction rate [kW]
ψ	specific flow exergy [kJkg^{-1}]

Subscripts

aec	inlet secondary fluid (condenser)
asc	outlet secondary fluid (condenser)
aee	inlet secondary fluid (evaporator)
ase	outlet secondary fluid (evaporator)
b	brine
$comp$	compressor
$cond$	condenser
dl	discharge line
$evap$	evaporator
ev	expansion valve
in	inlet
out	outlet
ref	refrigerant
1,2,3,...	thermodynamic state

References

- Ahamed, J.U., Saidur, R. and Masjuki, H.H. (2011). A review on exergy analysis of vapor compression refrigeration system. *Renewable and Sustainable Energy Reviews* 15, 1593-1600.
- Aminyavari, M., Najafi, B., Shirazi, A. and Rinaldi, F. (2014). Exergetic, economic and environmental (3E) analyses, and multi-objective optimization of a CO_2/NH_3 cascade refrigeration system. *Applied Thermal Engineering* 65, 42-50.
- Aprea, C., de Rossi F., Greco, A. and Renno, C. (2003). Refrigeration plant exergetic analysis varying the compressor capacity. *International Journal of Energy Research* 27, 653-669.
- Arora, A. and Kaushik, S.C. (2008). Theoretical analysis of a vapour compression refrigeration system with R502, R404A and R507A. *International Journal of Refrigeration* 31, 998-1005.
- Belegundu, A.D. and Chandrupatla, T.R. (2011). *Optimization concepts and applications in engineering*. Second edition, New York, Prentice Hall.
- Belman, J.M., Navarro-Esbrí, J., Ginestar, D. and Milian, V. (2010). Steady-state model of a variable speed vapor compression system using R134a as a working fluid. *International Journal of Energy Research* 34, 933-945.
- Chen, C.K. and Su, Y.F. (2005). Exergetic efficiency for an irreversible Brayton refrigeration cycle.

- International Journal of Thermal Sciences* 44, 303-310.
- Dinçer, I. and Kanoğlu, M. (2010). *Refrigeration Systems and Applications*. John Wiley and Sons Inc., United Kingdom.
- Dubey, M., Rajput, S.P.S., Nag, P.K. and Misra, R.D. (2010). Energy analysis of a coupled power-refrigeration cycle. *Journal of Power and Energy* 224, 749-759.
- Fábrega, F.M., Rossi, J.S. and d'Angelo, J.V.H. (2010). Exergetic analysis of the refrigeration system in ethylene and propylene production process. *Energy* 35, 1224-1231.
- Kalaiselvam, S. and Saravan, R. (2009). Exergy Analysis of scroll compressors working with R22, R407C, and R417A as refrigerant for HVAC system. *Thermal Science* 13, 175-184.
- Kizilkan, Ö., Kabul, A., Yakut, A.K. (2010). Exergetic performance assessment of a variable-speed R404a refrigeration system. *International Journal of Energy Research* 34, 463-475.
- Kotas, T.J. (1995). *The Exergy Method of Thermal Plant Analysis*. Malabar: Butterworths.
- Lugo-Leyte, R., Salazar-Pereyra, M., Ruíz-Ramírez, O.A., Zamora-Mata, J.M. and Torres-González, E.V. (2013). Exergoeconomic operation cost analysis to theoretical compression refrigeration cycle of HFC-134a. *Revista Mexicana de Ingeniería Química* 12, 361-370.
- Moran, M.J. and Shapiro, N.H. (2007). *Fundamentals of Engineering Thermodynamics*. 6th ed. Toronto, John Wiley and Sons, INC.
- Padilla, M., Revellin, R. and Bonjour, J. (2010). Exergy analysis of R413A as replacement of R12 in a domestic refrigeration system. *Energy Conversion and Management* 51, 2195-2201.
- Srinivasan, K., Lim, Y.K., Ho, J.C. and Wijesundera, N.E. (2003). Exergetic analysis of carbon dioxide vapour compression refrigeration cycle using the new fundamental equation of state. *Energy and Conversion Management* 44, 3267-3278.
- Su, Y.F. and Chen, C.K. (2006). Exergetic efficiency optimization of a refrigeration system with multi-irreversibilities. *Journal of Mechanical Engineering Science* 220, 1179-1187.
- Tao, Y.B., He, Y.L. and Tao, W.Q. (2010). Exergetic analysis of transcritical CO₂ residential air-conditioning system based on experimental data. *Applied Energy* 87, 3065-3072.
- Tsatsaronis, G. (1993). Thermoeconomic analysis and optimization of energy systems. *Progress in Energy and Combustion Science* 19, 227-257.
- Yumrutaş, R., Kunduz, R. and Kanoğlu M. (2002). Exergy analysis of vapor compression refrigeration systems. *Exergy, an International Journal* 2, 266-272.